24pW2-10

CALET observation of high-energy gamma-rays and toward better sensitivity above 100 GeV

# CALETによる高エネルギーガンマ線観測と100 GeV以上の領域の感度向上に向けて

立命館大理工, 早大理工総研[A],
NASA/GSFC[B], Louisiana State Univ.[C],
森正樹, 水野隼稀, 赤池陽水[A], 小林兼好[A],
鳥居祥二[A], N. Cannady[B],川久保雄太[C], M.L. Cherry[C],
他CALETチーム

M. Mori, T. Mizuno, Y. Akaike, K. Kobayashi, S. Torii, N. Cannady, Y. Kawakubo, M.L. Cherry for the CALET collaboration

日本物理学会2023年春季大会（オンライン）2023年3月22～25日

Cannady et al., ApJS 238:5 (2018)

# Gamma Ray Event Selection

**= Electron Selection Cut + Gamma-ray ID Cut w/ Lower Energy Extension**

## 100 GeV Event Examples

| gamma-ray | electron | proton |
|---|---|---|
| Charge Z=0 | Charge Z=1 | |

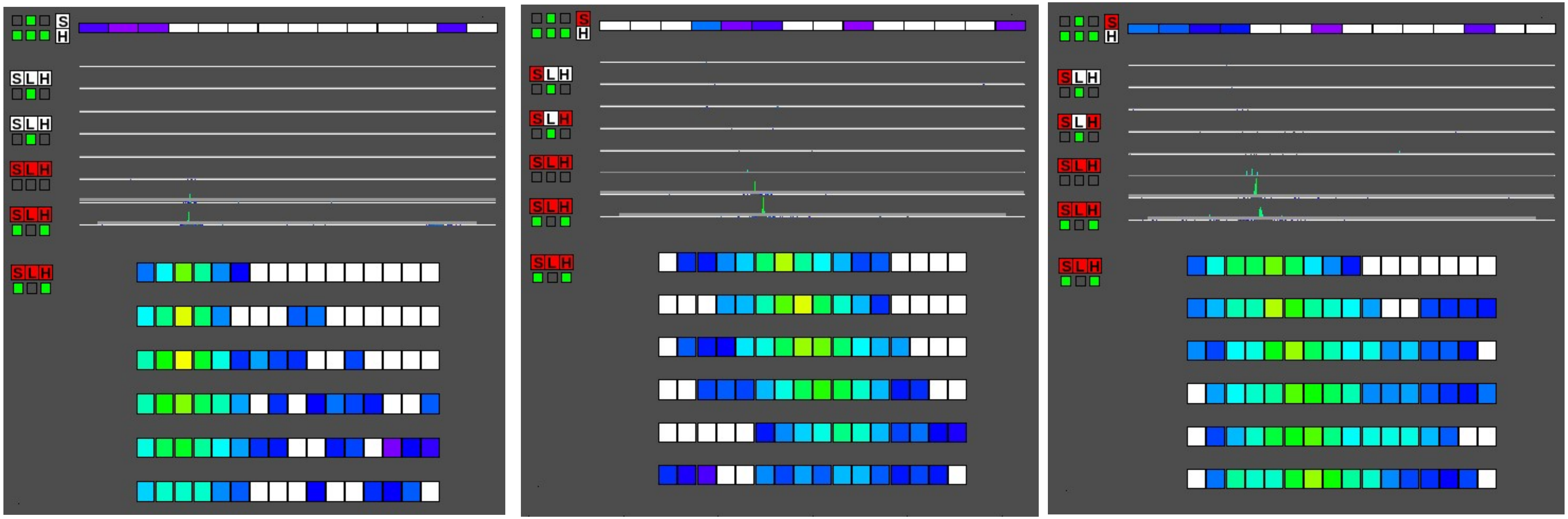

| Electromagnetic Shower | | Hadron Shower |
|---|---|---|
| well contained, constant shower development | | larger spread |

# CALET triggers and gamma-ray observation

Trigger rate vs ISS location

Asaoka et al., Astropart.Phys. 100, 29 (2018)

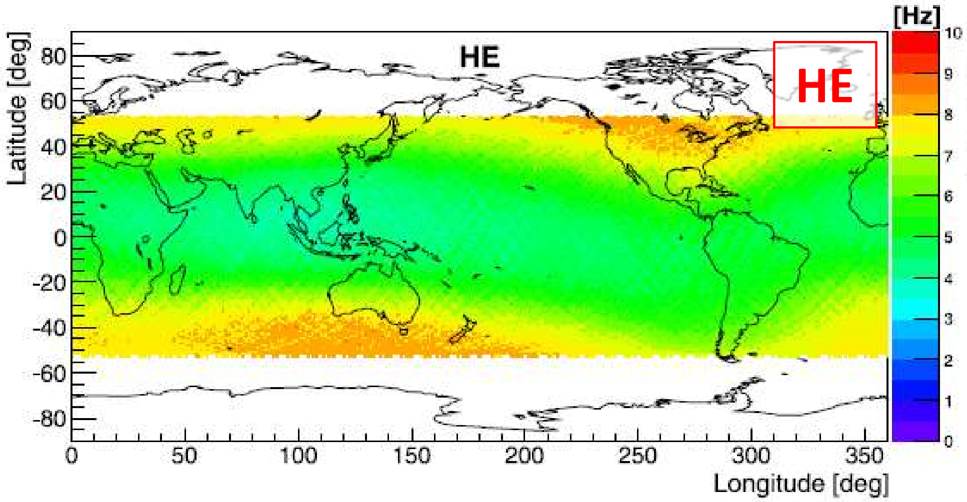


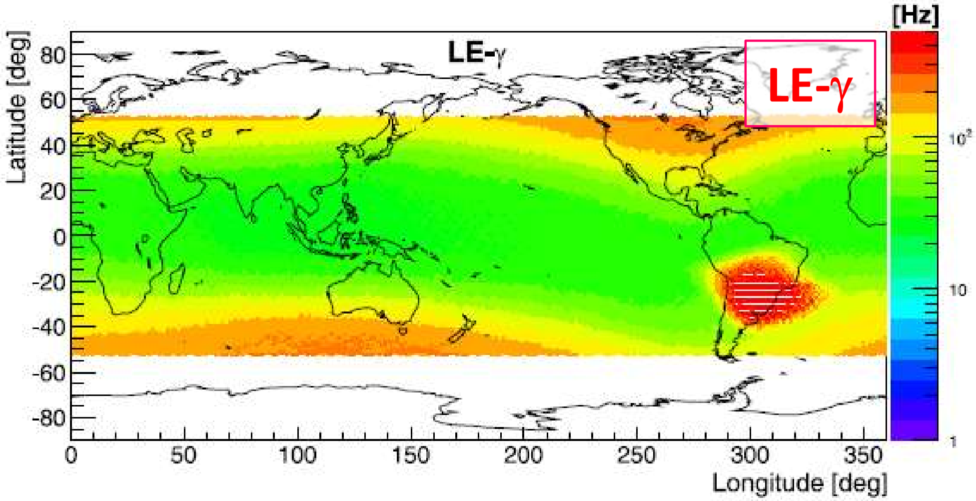


HE trigger: $E_\gamma$ > 10 GeV
LE-$\gamma$ trigger: $E_\gamma$ > 1 GeV

- HE trigger mode: always ON
- LE-$\gamma$ mode: ON when geomag.lat. < 20$^\circ$ or CALET Gamma-ray Burst Monitor (CGBM) is triggered

Typical operation

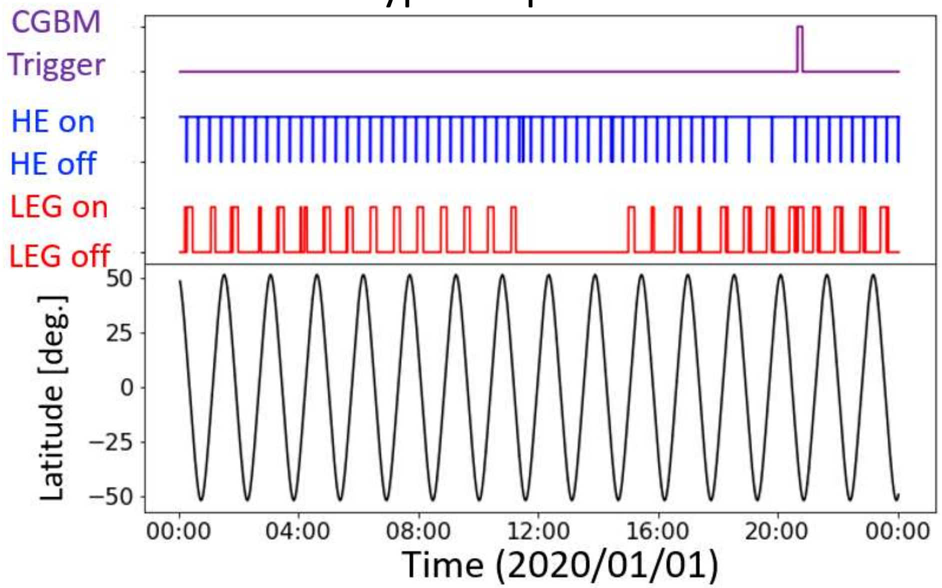

# CALET performance

- HE trigger (>10 GeV) is always active in normal observations
- LE-γ trigger (>1 GeV) mode is activated when the geomagnetic latitude is below 20° or following a CALET Gamma-ray Burst Monitor (CGBM) burst trigger

**Energy resolution**

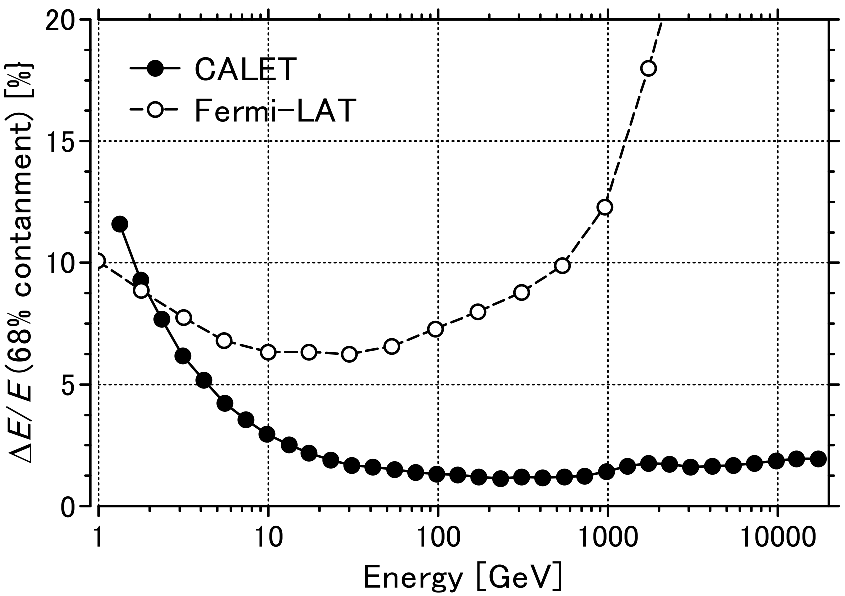


Asaoka et al, Astropart. Phys. 91, 1 (2017)

**Effective area (for gamma rays)**

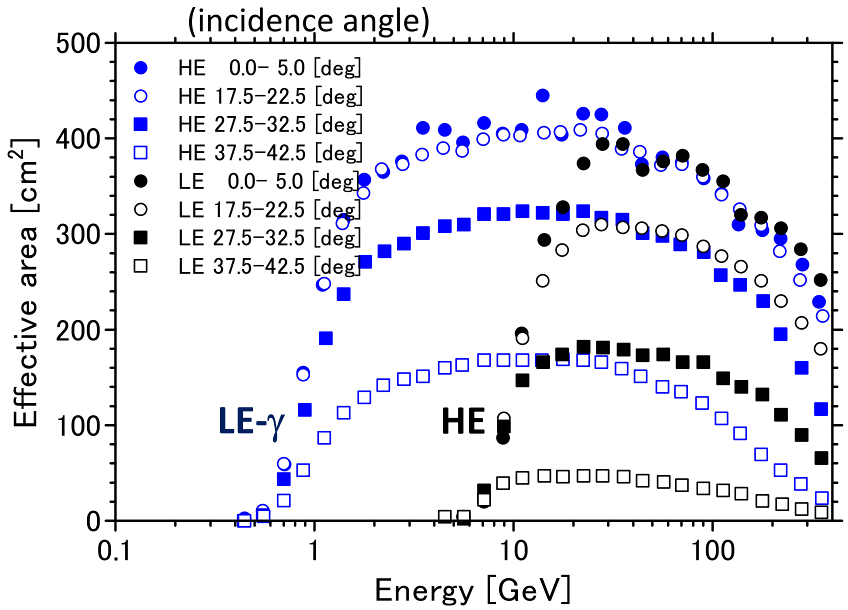


Cannady et al., ApJS 238, 5 (2018)

- Good energy resolution at high energies thanks to the thick calorimeter!

# Gamma-ray skymaps

November 2015 – February 2022

Preliminary

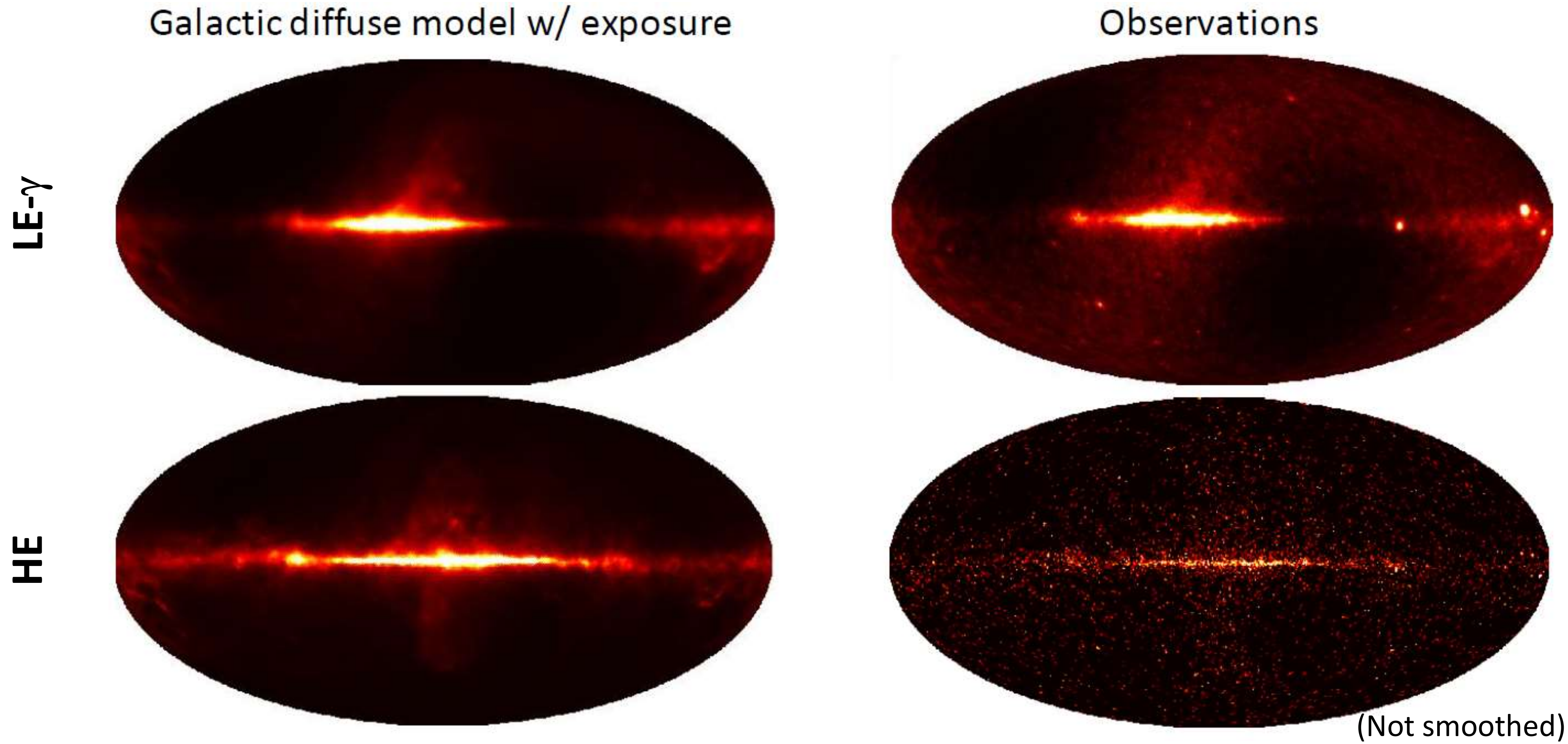


Note: Exposure is not uniform due to the ISS orbit (inclination 51.6°)

# Energy spectra for bright point sources

Preliminary

November 2015 – February 2022

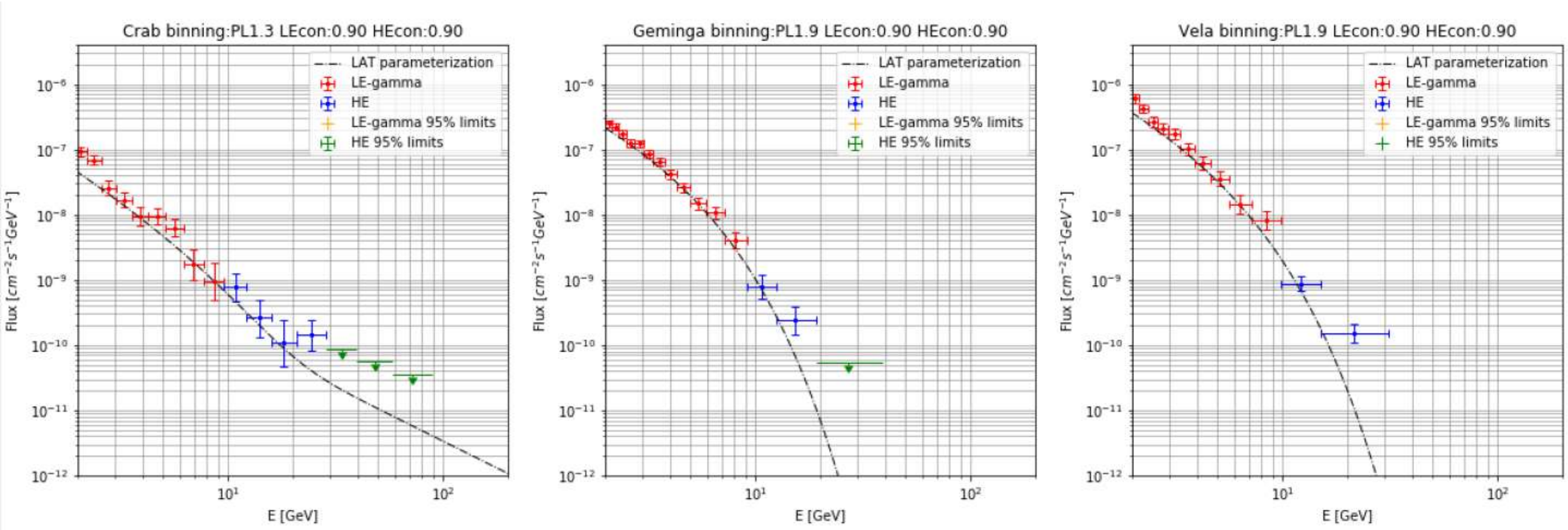


- Consistent with Fermi-LAT spectra

# Gamma-ray spectra (LE-γ & HE)

Preliminary

**LE-γ + HE** November 2015 – February 2022

(Fermi data: analyzed from public data.)

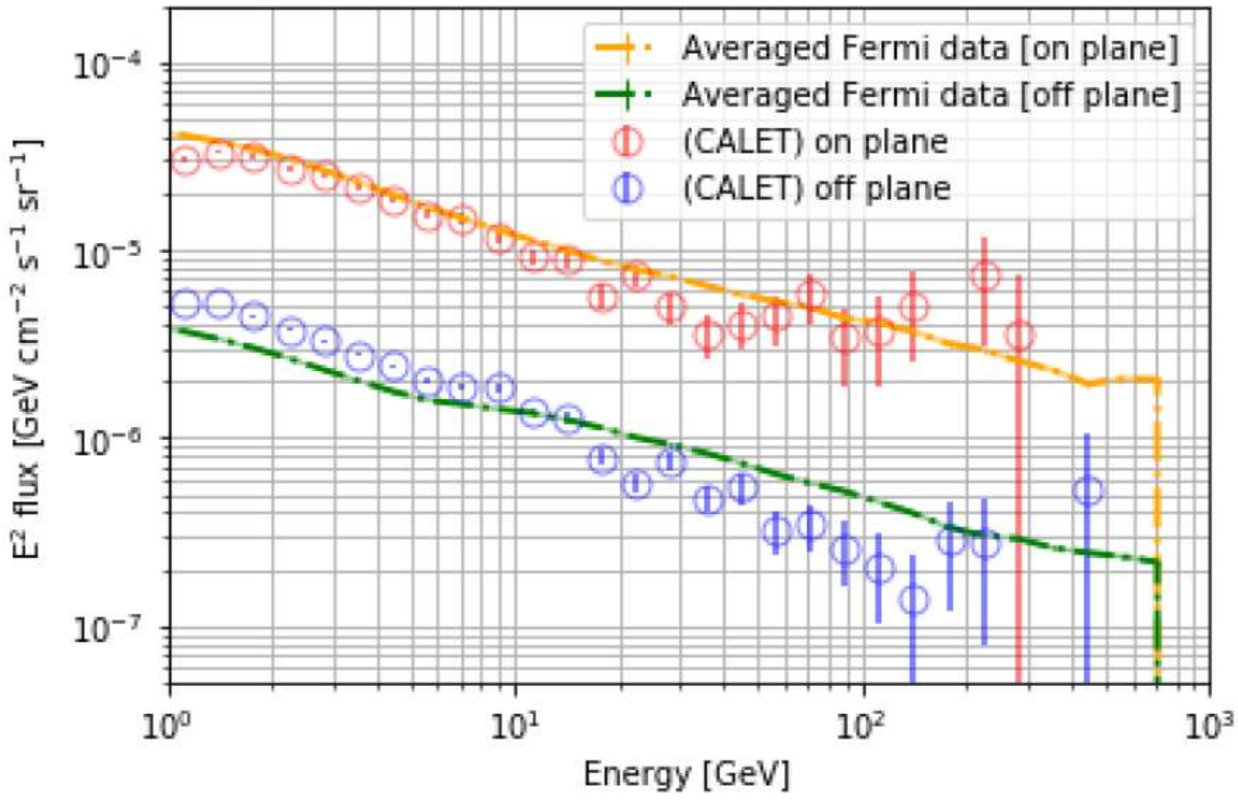


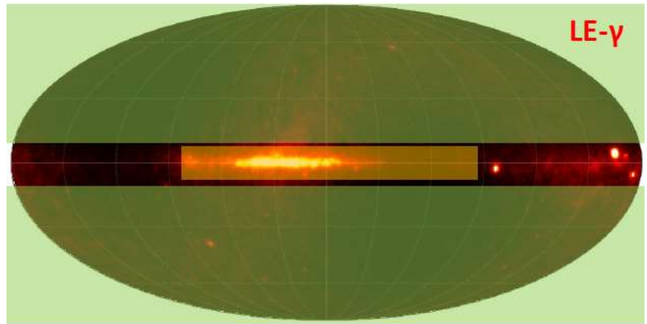


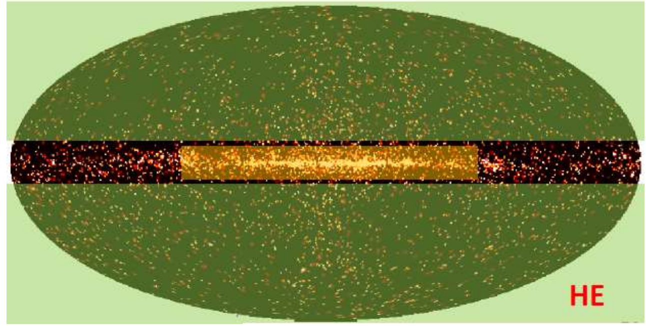


"**On-plane**": $|l| < 80°$ & $|b| < 8°$, "**Off-plane**": $|b| > 10°$

- The spectra (Galactic diffuse + point sources) look fairly consistent with those by Fermi-LAT.

# Transient follow-ups

- Trigger of CGBM instrument prompts CALET to temporarily activate LE-$\gamma$ mode to search for transient counterparts
- Transient analysis pipeline allows for quick follow-up of GRBs or LIGO/Virgo GW triggers
- Observations corresponding to triggers in LIGO/Virgo O3 run recently published in **Adriani et al., ApJ 933 85 (2022)**.
- Waiting for O4 to start…

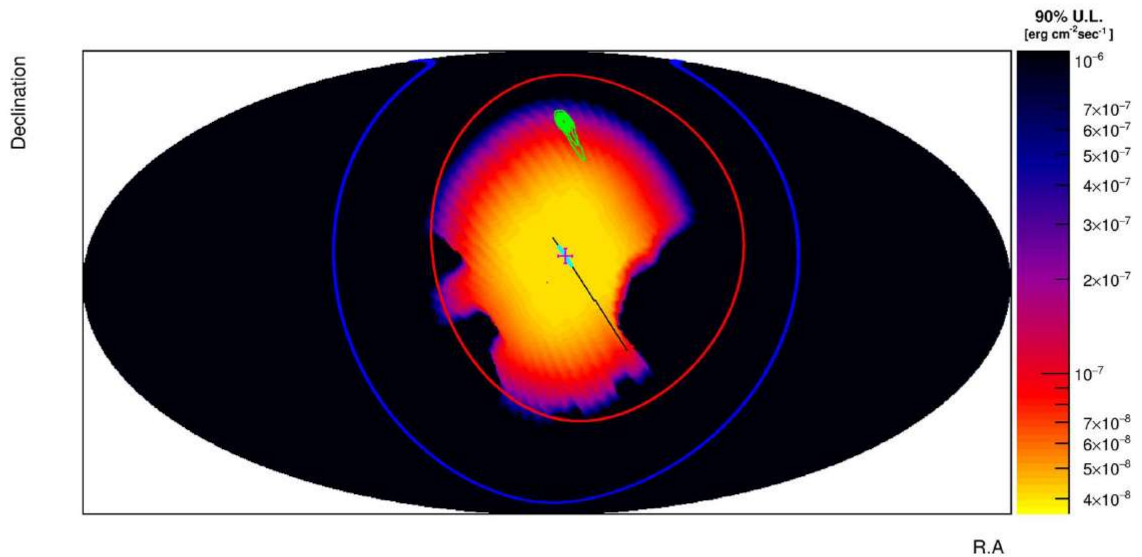


**Figure 10.** 90% confidence level upper limits observed by CAL in the energy range 1–10 GeV during the interval $\pm60$ s around the time of GW190408an reported by LIGO/Virgo. The intensity scale is given in units of erg cm$^{-2}$ s$^{-1}$. Red and blue circles are the HXM and SGM fields of view, respectively.

# Improvements to HE sensitivity (1)

- At higher energies, charge selection with CHD becomes contaminated with backscattered secondary particles.

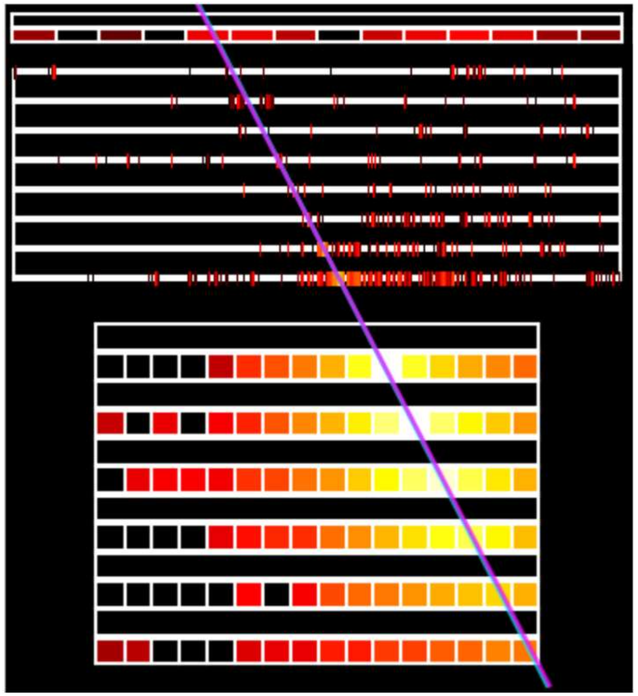

- New selection defined to use looser cuts in CHD and incorporating first two layers of IMC for charged primary rejection
- Preliminary results show significant increase in effective area *E* > 100 GeV
- Testing of selection and contamination being finalized for implementation in all analyses soon!

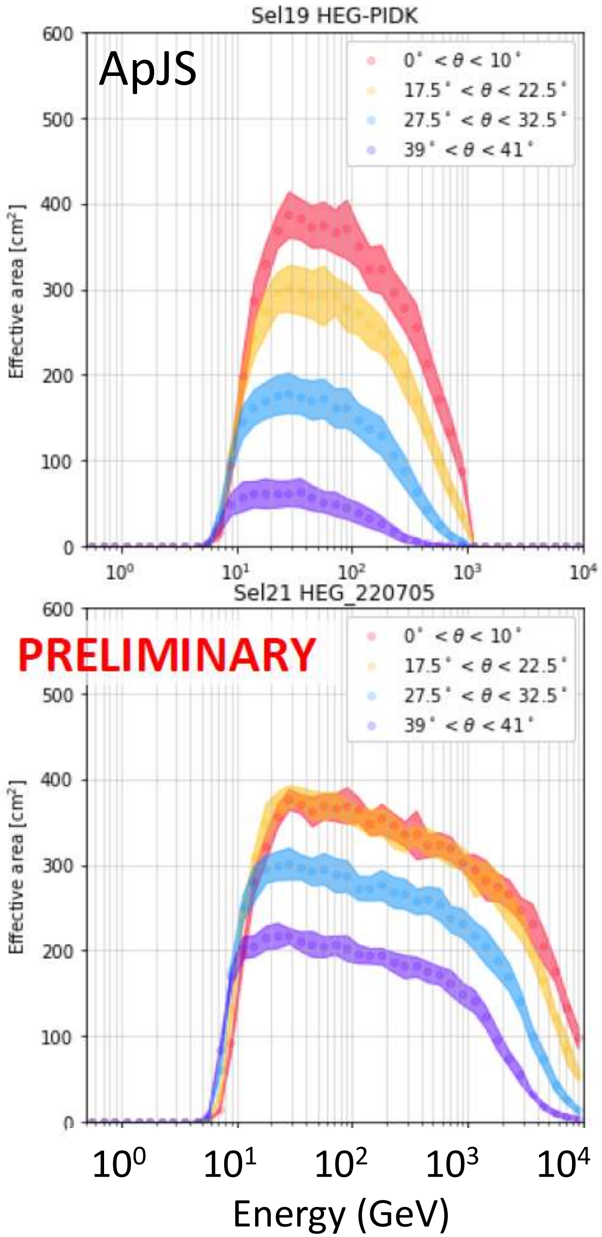

# Original (ApJS) definition of geometry E


| Acceptance | Conditions | | | Geom. Fact. $[cm^2 sr]$ |
|---|---|---|---|---|
| A | CHD top | TASC top* | TASC 6y bottom* | 419.1 |
| EB | CHD top | TASC top* | TASC 6y bottom | 91.03 |
| ED | CHD top | TASC top* | TASC path > 24 cm | 121.6 |
| EB3 | CHD top | TASC top* | TASC 3y bottom* | 51.97 |
| ED3 | CHD top | TASC top* | TASC 3y bottom | 127.9 |
| E | CHD top | TASC top* | | 373.8 |

Table 3.1: Requirements for the LE-$\gamma$ geometrical conditions. The conditions marked with asterisks denote that the intersection point must be more than 2 cm from the edge of the layer boundary.

**LE-$\gamma$ analysis uses A–E: total 1185.4 $cm^2sr$**
**HE analysis uses A–ED: total 631.73 $cm^2sr$**

**Compare to standard acceptance:**

| | Condition | SΩ[cm2sr] |
|---|---|---|
| A | CHD-X-top<br>&& CHD-Y-top<br>&& TASC-top (inside 1 log)<br>&& TASC-bot (inside 1 log) | A: 415.7 ± 1.1 |
| B | CHD-X-top<br>&& CHD-Y-top<br>&& TASC-top<br>&& TASC-bot<br>&& !{ TASC-top (inside 1log)<br>&& TASC-bot (inside 1log) } | B: 154.6±0.7<br>A+B: 570.3±1.3 |
| C | IMC5th layer<br>&& TASC-top<br>&& TASC-bot<br>&& !{ CHD-X-top<br>&& CHD-Y-top } | C: 230.1±0.8<br>A+B+C: 800.4±1.6 |
| D | IMC5th layer<br>&& TASC-top<br>&& path length in TASC > thickness of TASC<br>&& !TASC-bot | D: 236.4±0.8<br>A+B+C+D:1036.6±1.8 |

# Revised definition of geometry E


| Acceptance | Conditions | | | Geom. Fact. $[cm^2 sr]$ | |
|---|---|---|---|---|---|
| A | CHD top | TASC top* | TASC 6y bottom* | 419.11 | 419.11 |
| EB | CHD top | TASC top* | TASC 6y bottom | 91.03 | 510.14 |
| ED | CHD top | TASC top* | TASC path > 24 cm | 121.55 | 631.69 |
| EB3 | CHD top | TASC top* | TASC 3y bottom* | 51.97 | 683.65 |
| ED3 | CHD top | TASC top* | TASC 3y bottom | 127.94 | 811.59 |
| E | CHD top | TASC top* | | 372.81 | 1184.4 |

Table 3.1: Requirements for the LE-γ geometrical conditions. The conditions marked with asterisks denote that the intersection point must be more than 2 cm from the edge of the layer boundary.

Should have been <u>bottom of TASC X1 rather than top</u> for better containment

exclusive

cumulative

Better energy resolution for only small change in geometrical factor:

| Acceptance | Conditions | | | Geom. Fact. $[cm^2 sr]$ | |
|---|---|---|---|---|---|
| A | CHD top | TASC top* | TASC 6y bottom* | 419.11 | 419.11 |
| EB | CHD top | TASC X1 bot* | TASC 6y bottom | 99.20 | 518.31 |
| ED | CHD top | TASC X1 bot* | TASC path > 24 cm | 122.16 | 640.57 |
| EB3 | CHD top | TASC X1 bot* | TASC 3y bottom* | 53.26 | 693.72 |
| ED3 | CHD top | TASC X1 bot* | TASC 3y bottom | 125.78 | 819.51 |
| E | CHD top | TASC X1 bot* | | 277.17 | 1096.68 |

Table 3.1: Requirements for the LE-γ geometrical conditions. The conditions marked with asterisks denote that the intersection point must be more than 2 cm from the edge of the layer boundary.

# Improvements to HE sensitivity (2)

‘**RitsumeiGamma**’ selection

For events with definite tracks (same as CaletGamma)

Preselection

| | |
|---|---|
| TASCgeometry ① | Selection based on distance between energy-COG and track |
| TASClength ② | Selection based on distance travelled in TASC |
| CHDarea ③ | Selection based on passing through CHD |

Gammaselection

Gamma ray selection with/without CHD signal

Gamma ray | Not gamma ray

(Geometry just matches to CALET ‘ED’)

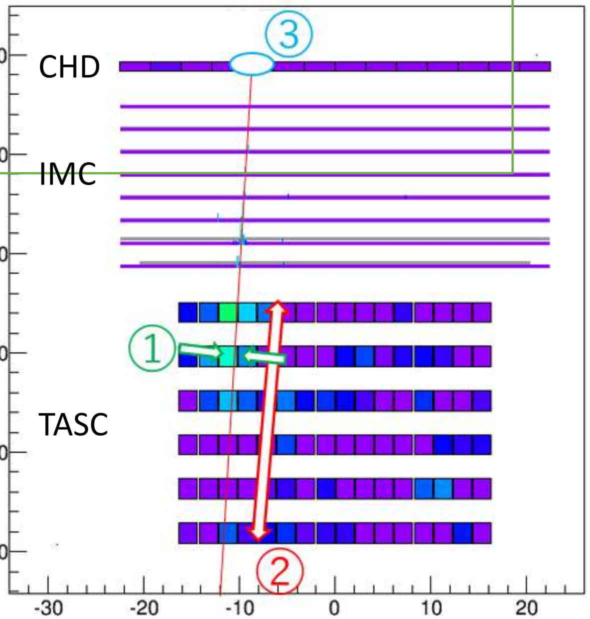


*This selection puts more weight in TASC energy deposit.*

# MC datasets

- COSMOS 8.039/EPICS 9.28
- Set A
  - Fixed direction (zenith 19.5°, azimuth 30°)
  - Fixed position (passing the center of TASC top)
  - Energy: $10^{1.4} – 10^{3.6}$ GeV ($10^{0.2}$ step), 20,000 events each
- Set B
  - Uniform direction (zenith 0 – 60°, azimuth 0 – 360°)
  - Uniform position (55cm×55cm above 2cm of CHD top)
  - Energy: $10^{1.4} – 10^{3.6}$ GeV ($10^{0.2}$ step), 200,000 events each

# Comparison of ‘RitsumeiGamma’ with ‘CaletGamma’

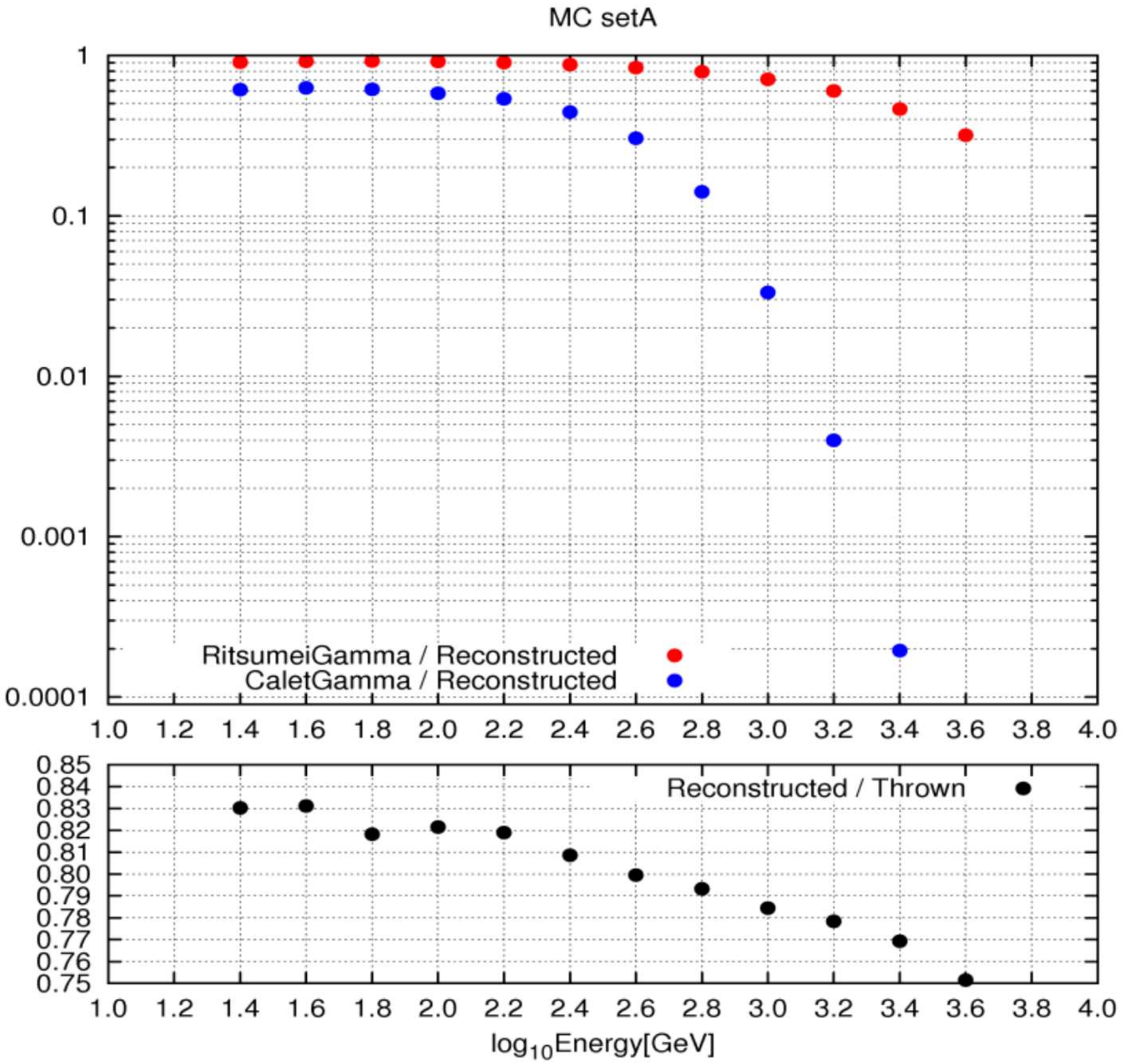


Set A

# Comparison of ‘RitsumeiGamma’ with ‘CaletGamma’

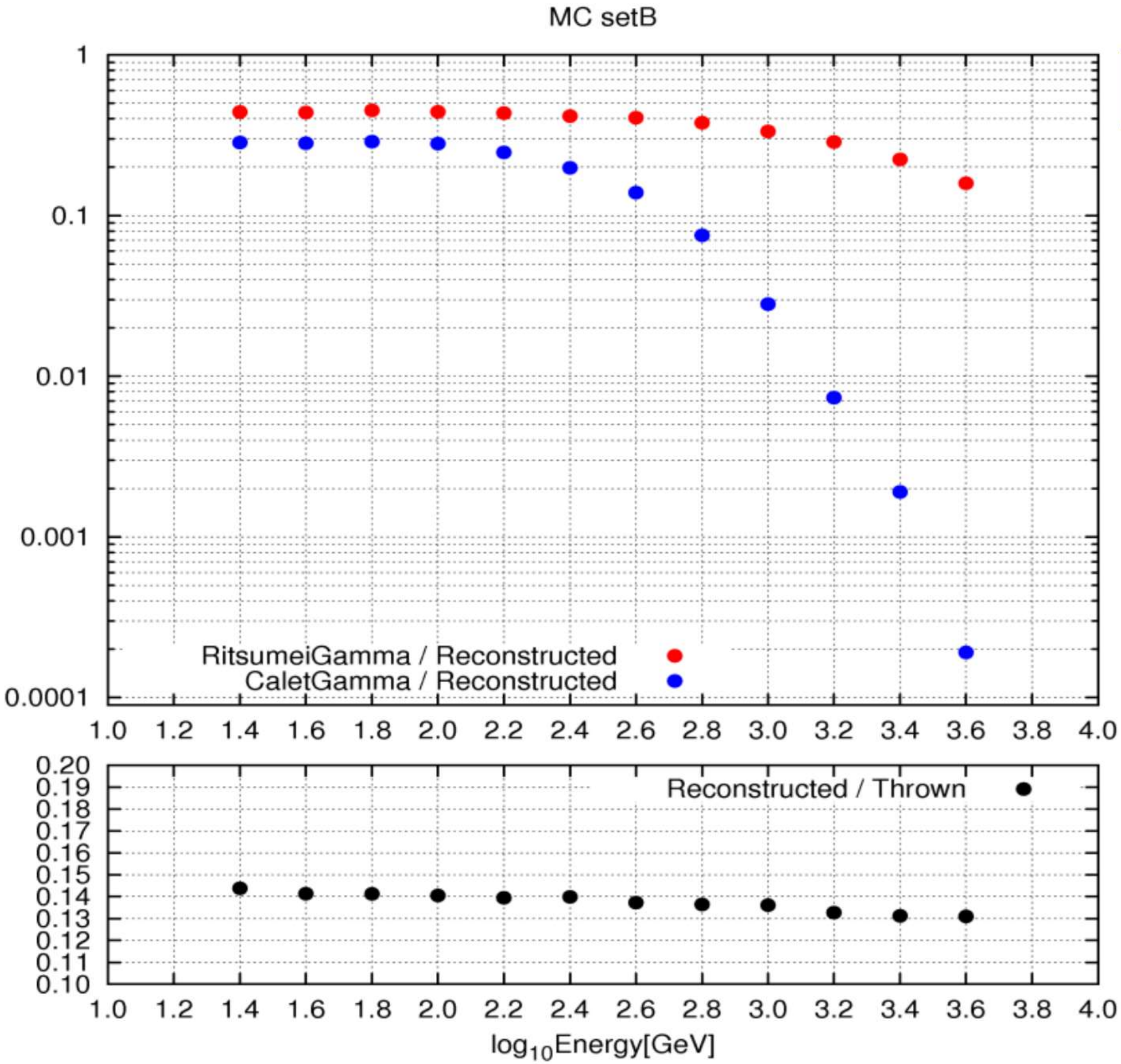


Set B

# Opening angle (between true and reconstructed) distribution

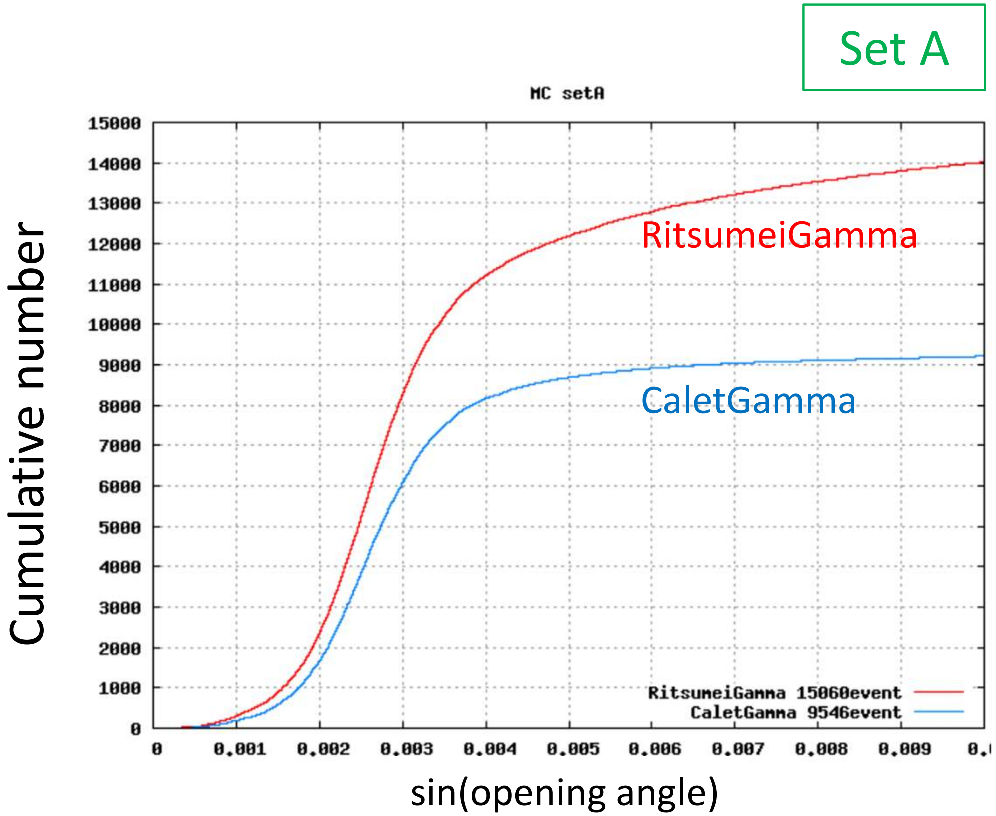


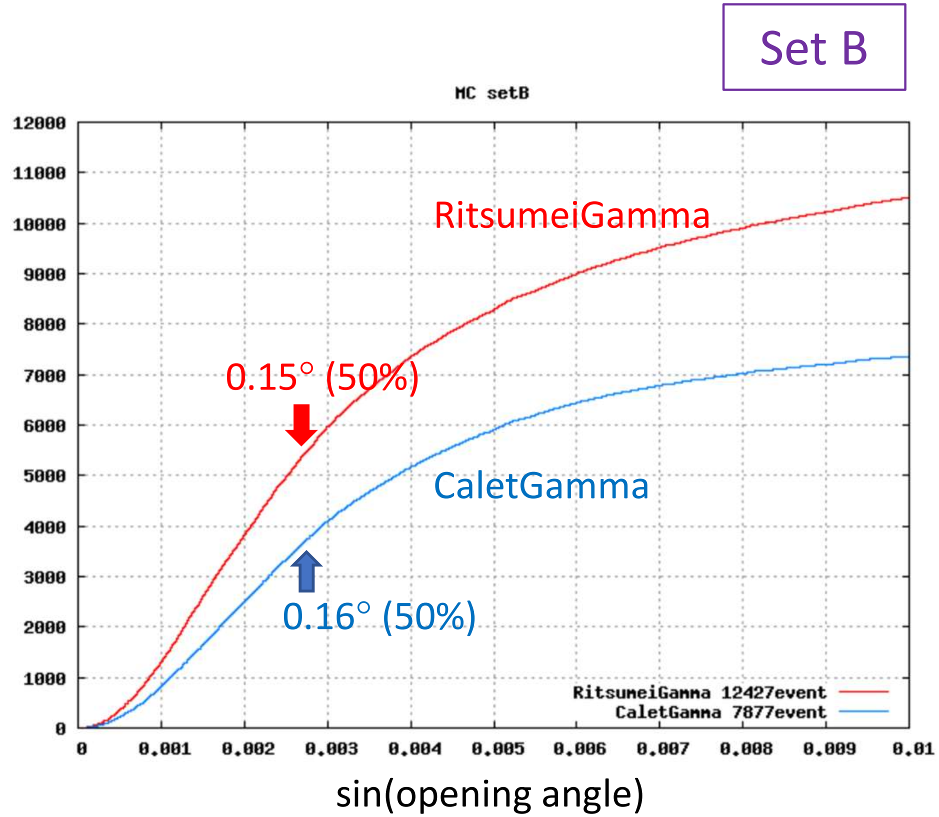


Angular resolution is similar but slightly better in RitsumeiGamma.

# Summary

- CALET has been observing celestial gamma ray above 1 GeV for more than 7 years since its launch in October 2015.
- Improvements to high-energy (>100 GeV) sensitivities are going on…
  - Present analysis is optimized for the GeV energy range.
  - Significant increase in effective area is expected in the 100 GeV region with the new analysis under development if applied to Monte Carlo data.
  - Next, we try to apply the new analysis to flight data.